Published in IET Communications
Received on 23rd November 2008
Revised on 15th March 2009
doi: 10.1049/iet-com.2008.0674

ISSN 1751-8628

Directional modelling of ultra wideband communication channels

A.H. Muqaibel

Electrical Engineering Department, King Fahd University of Petroleum & Minerals, P.O. Box 1734, Dhahran 31261, Saudi Arabia
E-mail: muqaibel@kfupm.edu.sa

Abstract: Ultra wideband (UWB) propagation is antenna-dependent, and multipath components experiencing specular diffraction or arriving at different angles have different shapes. To utilise the diversity of the multipath components, this study proposes a statistical model which incorporates directional parameters, such as elevation and azimuth angles by extending the IEEE802.15.3a model. Based on this model, a UWB directional simulator is developed. A novel multi-template subtractive deconvolution is applied to an extensive measurement campaign and simulated profiles. The use of multi-templates makes possible the directional estimation of the multipath components with a single receive antenna, and the use of subtractive deconvolution allows for the resolution of overlapping components and higher energy capture. Directional characterisation of UWB channels facilitates performance evaluation studies and achieves more accurate positioning, imaging and Rake receiver design.

1 Introduction

Ultra wideband (UWB) devices are usually defined as any device whose emissions have a fractional bandwidth greater than 0.2 or occupy more than 0.5 GHz of spectrum [1]. Other researchers define UWB as electromagnetic waves with instantaneous bandwidth greater than 25% of centre frequency [2].

UWB technology is a potential candidate for short-range multiple access wireless communication applications, including indoor static wireless local area networks (LANs) [3], decentralised multiple access communication and secure military applications [4]. Besides communication applications, UWB can be used for range measurements [5]. UWB receivers can time the transmitted pulses to within a fraction of a pico-second. This potential of UWB technology underpins its distinctive capabilities. It can support high transmission rates, has excellent wall penetration capabilities and consumes very low power.

Due to the rapidly growing interest in UWB communications, researchers have devoted considerable efforts and resources to develop robust channel models (CMs) to allow for reliable and accurate UWB performance evaluation. A summary of some temporal UWB characterisation research on both deterministic and statistical modelling is provided in [6]. All temporal results account for frequency-dependent antenna characteristics.

In addition to the temporal characterisation, some researchers have attempted directional UWB characterisations. For example, diversity is considered by the researchers in [7] to extract the structure of the channel from the received array of data. Beam former response at different projection angles has also been studied. Prettie *et al.* [8] have presented spatial correlation of UWB measurements.

To illustrate the importance of directional models, Cramer *et al.* [7] suggested modelling the UWB channel as a summation of the Hermite polynomials. Their justification was based on the heuristic approach that the signal driving the antenna is often modelled as Gaussian, and some of the propagation and reflection effects tend to have the characteristics of the signal derivatives. Later studies revealed that derivative behaviour is a result of the specific antenna transfer function [9].

Some recent publications concentrated on spatial correlation in the receiver antenna arrays [10]. Multi-input multi-output systems can exploit the antenna arrays to enhance the data rate. The work of [11] compared the channel parameters when using directional and omni-directional antennas. In [12] an attempt was made to extract the transfer function for transmit and receive antennas from the overall channel measurement or simulation. The idea is based on the derivative relation between the transfer functions of transmit and receive antennas under certain conditions.

There are some directional narrowband/wideband models [13, 14], but none was developed with UWB communication in mind. The directional issue is very important because of the fact that UWB propagation is antenna-dependent. The spectrum and the shape of the pulse also affect the propagation. A directional model should include the angle of transmission and the angle of arrival. UWB multipath components received at different angles have different shapes.

The main contribution of the present research may therefore be identified as the proposal of a statistical UWB propagation model, taking account of the directional nature of UWB propagation, that is transmit and receive antennas. The proposed model is based on the temporal model of Saleh and Valenzuela [15], extended and approved by the IEEE802.15.3a standard, and on the wideband statistical directional model proposed by Spencer *et al.* [13]. A directional simulator, which incorporates the suggested statistical model, is developed. This simulator is used to generate a data bank of multipath profiles. The paper also analyses two different signal-processing techniques for multipath extraction; namely, zero-insertion and subtractive deconvolution. The proposed signal-processing techniques are applied to both experimental and simulated data.

In light of the future of the very promising UWB technology, the objective of this study is directional UWB channel characterisation. Since the existing statistical UWB CMs do not incorporate the effect of the antenna, the present study considers the possibility of extending the existing wideband directional models to UWB systems. This should allow the study of the multipath performance at different angles. The outcome of this investigation can be utilised to improve the design of UWB receivers, the accuracy of channel characterisation and it should be valuable for positioning applications.

The remaining part of the paper is structured in the following way. Section 2 proposes a statistical directional UWB CM. In Section 3, the proposed model is implemented using an antenna-aware statistical simulator. In Section 4, the signal-processing used to extract the channel parameters from the channel impulse response is analysed and enhanced. Section 5 presents the results. The paper ends with some concluding remarks.

2 Proposed directional UWB channel model

When the channel is excited with a pulse, the received waveform is a summation of modified pulses with different attenuation factors, α_k, and different time delays, τ_k, where k is the path index. The received waveform is referred to as a multipath profile, and the individual pulses are referred to as multipath components because they arrive at the receiver through different paths.

For narrowband systems, no dispersion within individual pulses may be assumed, and hence the channel impulse response is real and can be represented as a superposition of these paths as in (1).

$$h(t) = \sum_k \alpha_k \delta(t - \tau_k) \tag{1}$$

where $\delta(\cdot)$ is the Dirac delta function. The excess delay, τ_k, is a measure of time delay relative to the first arriving component.

The signal at the receiver, $r(t)$, is the time convolution of the generated pulse, $p(t)$, and the overall channel impulse response, $h(t)$. This received signal is given by

$$r(t) = \sum_k \alpha_k p(t - \tau_k) \tag{2}$$

Narrowband communication is usually achieved by modulating a sinusoidal carrier with the information to be transmitted. The resultant signal has a sinusoidal nature, and occupies a narrow band in the frequency domain. On the other hand, for UWB applications, any waveform that satisfies the definition of UWB signal can be used. The choice of a specific waveform is driven by system design and application requirements. The IEEE 802.15.3a model, based on Saleh–Valenzuela model [15], is usually used for modelling UWB channels. Based on experimental analysis, the IEEE 802.15.3a model uses a lognormal distribution rather than Rayleigh distribution for the multipath gain magnitude [16]. Also, independent fading is assumed for each cluster as well as for each ray within the cluster. The assumption of no-dispersion is not acceptable for UWB signals, because of the frequency-selective nature of the transfer function of the overall communication channel. Thus, there is a need to extend the model developed by the IEEE 802.15.3a working group [16] by incorporating the directional nature of the channel.

The IEEE 802.15.3a model is given by

$$h_i(t) = X_i \sum_{l=0}^{L} \sum_{k=0}^{K} \alpha_{k,l}^i \delta\left(t - T_l^i - \tau_{k,l}^i\right) \tag{3}$$

where $\alpha_{k,l}^i$ is the multipath gain coefficient, T_l^i is the delay of lth cluster, $\tau_{k,l}^i$ is the delay of the kth multipath component

doi: 10.1049/iet-com.2008.0674

relative to the lth cluster-arrival time, X_i represents lognormal shadowing where the subscript i refers to the ith realisation, T_l is the arrival time of the first path of the first cluster and $\tau_{k,l}$ is delay of the kth path in the lth cluster relative to T_l. By definition $\tau_{0,1} = 0$.

The arrival times are given by exponential distributions with Λ as the cluster-arrival rate and λ as the ray-arrival rate.

The time components of the model are derived from two independent distributions. The distribution of the coefficients related to the magnitude of the received multipath component can be found in [16].

The directional nature of the multipath components is not a major issue in narrowband systems; but this is not the case for wideband systems. For example, Klein and Mohr [14] presented a statistical wideband mobile radio CM including the directions-of-arrival. Their model was derived by extending conventional statistical tap-delay-line models of the mobile radio channel to take into account the direction of arrival.

A similar attempt was made by the researchers in [13] where a combined temporal/spatial statistical model for indoor multipath propagation was presented on the basis of a modified version of Saleh–Valenzuela model. The combined model is given by [13]

$$h(t, \theta) = \sum_{l=0}^{\infty} \sum_{k=0}^{\infty} \beta_{kl} e^{j\phi_{kl}} \delta(t - T_l - \tau_{kl}) \delta(\theta - \Theta_l - \omega_{kl}) \tag{4}$$

The $e^{j\phi_{kl}}$ term represents a statistically independent random phase with each arrival, where ϕ_{kl} is uniform on $[0, 2\pi)$. The amplitude of each arrival is given by β_{kl}, which is assumed to be a Rayleigh-distributed random variable. It is proposed that the angle of arrival be characterised by a cluster angle Θ_l and a ray angle ω_{kl}. It is also assumed that the cluster statistics are independent of the ray statistics in both time and space. The time and angle of the first arrival are heavily dependent on the specific room geometry. In order to eliminate this dependence, all measurements are made with respect to the first arrival. The cluster-arrival angle, relative to the first arrival, is approximately uniform on the interval $[0, 2\pi)$. The ray angle is assumed to have a zero-mean Laplacian distribution with standard deviation σ and is given by [13]

$$p(\omega_{kl}) = \frac{1}{\sqrt{2}\sigma} e^{-|\sqrt{2}\omega_{kl}/\sigma|} \tag{5}$$

It is further assumed that the time and angle-of-arrival characteristics are independent. The justification of the Laplacian model used by [13] is based on their wideband measurement campaign.

The above-mentioned models do not take into consideration the separate angles of the transmitter and receiver antennas. To extend the wideband model to UWB communication, it is important to separate the angles of the transmitter and the receiver antennas. This is because the transmitter and receiver antennas have their own orientation and reference coordinates. Assume that θ_t and φ_t refer respectively to the vertical and horizontal angles for the transmitted ray. Similarly, θ_r and φ_r refer to the vertical and horizontal angles at which the ray is received. Now, the directional impulse response is given by $h(t, \theta_t, \varphi_t, \theta_r, \varphi_r)$.

One possible simplification is to consider the relative angle between the transmitted and the received rays, regardless of whether the multipath component arrives on a direct line-of-sight (LOS) path or via scattering. The relative vertical and horizontal angles are referred to as θ and φ, respectively. This simplification is useful if we assume that the channel is composed of ideal specular reflectors. Now, the directional impulse response is given by $h(t, \theta, \varphi)$ and the IEEE802.15.3a model can be modified so that it will be as follows.

$$h_i(t, \theta, \varphi) = X_i \sum_{l=0}^{L} \sum_{k=0}^{K} \alpha_{k,l}^i \delta\left(t - T_l^i - \tau_{k,l}^i\right) \delta\left(\theta - \Theta_l^i - \omega_{k,l}^i\right) \times \delta\left(\varphi - \Phi_l^i - \upsilon_{k,l}^i\right) \tag{6}$$

where Θ is the cluster vertical (elevation) angle with uniform distribution on $[0, \pi)$; ω is the ray vertical angle with zero-mean Laplacian distribution and standard deviation σ_ω; Φ is the cluster horizontal (azimuth) angle with uniform distribution on $[0, 2\pi)$ and υ is the ray horizontal angle with zero-mean Laplacian distribution and standard deviation σ_υ.

Equation (6) represents the proposed directional UWB CM. In the next section, the simulation of the proposed model is discussed.

3 Statistical and directional transverse electromagnet-based UWB simulator and measurements in hand

In [17], the researchers developed an UWB simulator that uses transverse electromagnetic (TEM) horn antennas at the transmitter and the receiver. Horn antennas were used because the available experimental data were carried out on a communication system that utilised the TEM horn antennas and because this antenna could meet the UWB design considerations.

Two routines were developed to implement the directional transfer function for the transmit and receive antennas. The first routine calculated the radiated field

from a TEM horn antenna in any observation point in space for a given excitation voltage. The second routine calculated the received voltage at the output terminals of a TEM horn antenna because of an arbitrary incident electric field. To implement the proposed model in (6), the two routines were linked by a main program that contains the CM. The simulator, which was originally designed for theoretical input signals and deterministic channels, was upgraded to accept arbitrary signals and implement the proposed CM. The model parameters suggested by the working group, which are classified into four sets CM1 through CM4, can be found in [18]. There are different sets of parameter values to represent different channel characteristics. When the simulation bank was generated, the targeted channel characteristics were channel CM1 for LOS scenarios and CM2 for non-line-of-sight (NLOS). The code for the IEEE802.15.3a temporal model is available in [19] but was rebuilt and tested by the present author. For the directional part of the model, we used $\sigma_\omega = \sigma_\upsilon = 22^\circ$. This value of the standard deviations was used by Spencer *et al.*, [13] and it reflects the fact that most of the ray-arrival angles are within a few degrees of the clustered arrival. Another practical parameter in simulation is to decide when to limit the profiles, as theoretically the profile can extend in time for ever. NP is defined as the number of time constants before the profile is assumed to have decayed to zero. The larger the value of NP, the longer the data and processing time required. When the profiles were generated, NP was traded off to provide efficient processing. NP = 1, 3 and 5 were examined.

The simulator was fed with the realistic input signal illustrated in Fig. 1. This allows the simulation to be compared with the available field measurements. The channel-simulator calculates the number of multipath components, their amplitude, their time-of-arrival, and their elevation and azimuth angles. The antenna–simulator [17] is then run for each case of these multipath components, and the results are superimposed to find the total received voltage at the terminal of the receiving antenna. The generated data bank consists of 200 LOS and 50 NLOS profiles.

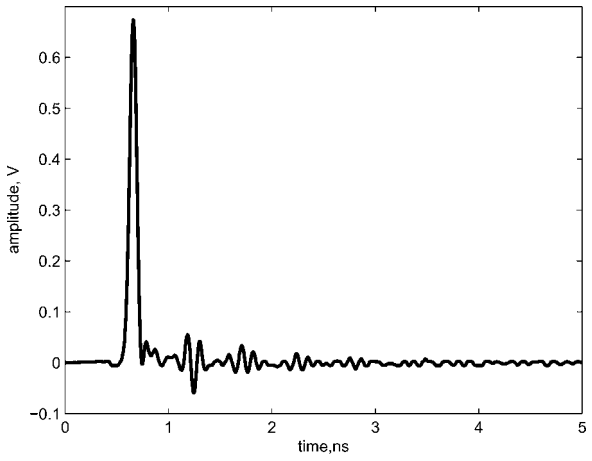

Figure 1 *Measured real input signal to the transmitting TEM horn antenna*

In addition to the simulated bank of profiles, a set of measured profiles is also available to validate the results. UWB channels were measured in the time domain by sounding the channel with pulses to obtain the impulse response. The setup used consists of a pulse generator that sends impulses to a TEM horn transmitting antenna through a balun. The received signal was observed by the use of a digitising oscilloscope. The receive antenna is also a TEM horn connected to the test set through a balun. The 3-dB bandwidth for the pair of antennas is 1–7 GHz. The sampling oscilloscope was connected to a data acquisition unit. Synchronisation was achieved through an external circuit.

The measurements were carried out in two buildings on Virginia Tech Campus, USA. The first building comprises mainly offices and classrooms with most walls made of drywalls with metallic studs. Some walls at certain locations including stairwells are made of cinderblock and poured concrete. The second building has interior walls which are mainly made of drywalls and cinderblocks. The floor is covered with carpet inside the rooms and with tiles in the hallways.

Altogether, 186 multipath profiles were examined. NLOS scenarios comprised 61 profiles. The remaining 125 profiles were LOS profiles. Every profile extended for 150 ns with 10 ps sampling interval. The pulse generator provided Gaussian-like pulses with a full-width half-maximum duration of 85 ps. More details about the measurements and data acquisition can be found in [20].

4 Signal-processing and Rake receiver design

Given the measured or simulated data, one has to employ signal-processing techniques to extract the channel parameters. The early characterisation attempts reported in the literature extend the narrowband measurement scenarios to the UWB case. Both the approach and the results need to be verified.

For narrowband characterisation, usually no deconvolution is needed, and the received signal can approximate the impulse response. Deconvolution was used only when super-resolutions were required [21, 22]. Deconvolution is most needed for the characterisation of wideband devices and channels, because of the limited bandwidths of available test signals compared to the bandwidths of devices and channels themselves [23]. Since the channel under study is wideband, deconvolution techniques are needed to estimate the UWB channel impulse response. Moreover,

doi: 10.1049/iet-com.2008.0674

with deconvolution, the estimated channel impulse response is independent of the excitation signal, which allows for the simulation of different waveforms for wave-shaping studies.

Since the radiation pattern of the antenna varies with frequency, UWB multipath components that are transmitted and received at different angles will have different shapes. Usually directional channel characterisation requires antenna arrays. This research proposes to utilise the diversity of the waveforms to extract the relative direction of arrival with a single antenna. Multi-template subtractive deconvolution is proposed in order to utilise the variation of the waveforms to extract the directional UWB channel response.

In the next subsection, the modified multi-template deconvolution algorithm is formalised, and then directional information about the channel is extracted. Finally, some conclusions are derived.

4.1 Multi-template subtractive against zero-insertion deconvolution

Channels can be characterised by their transfer function in the frequency domain or by their impulse response in the time domain. The measured and simulated profiles are represented in the time domain. Deconvolution of the time-domain waveforms can be used to determine the impulse response of a linear time-invariant system.

Although the transfer function and the impulse response provide a full channel description, only a few parameters can be used by the receiver for channel estimation. Model deconvolution is usually used to characterise the channel with few parameters [24].

The impulse response of the narrowband propagation channel is often modelled as a summation of delayed and scaled multipath components. This model does not fit the UWB channel, because the delta function at the receiver implies a wide channel bandwidth relative to the bandwidth of the excitation pulse. The sounding pulse, the transmitter and receiver antennas, and the impulse response of the detector must be deconvolved from the received profile [9].

For the measurements in hand, since the transmitter and the receiver antennas do not have spherical patterns at all frequencies, the waveforms received at different angles look considerably different. Fig. 2 illustrates a simple scenario where the transmitter and the receiver are facing each other and the receiver elevation angle is rotated in 15° steps. Both measured and simulated signals are presented in Fig. 2. There are some differences between the simulated and the measured templates, mainly because the simulated antenna transfer function does not fully model the measured antenna. Due to the symmetry of the antenna, positive and negative angles result in the same pulse shape. The proposed CM will be used next to account for the variation of the received waveforms.

The received profiles are composed of scaled and delayed pulses of different shapes depending on the angles of transmission and reception. We will discretise the angles and assume a finite number of possible templates, $\hat{p}^j(t)$ where $j = 1, 2, \ldots M$.

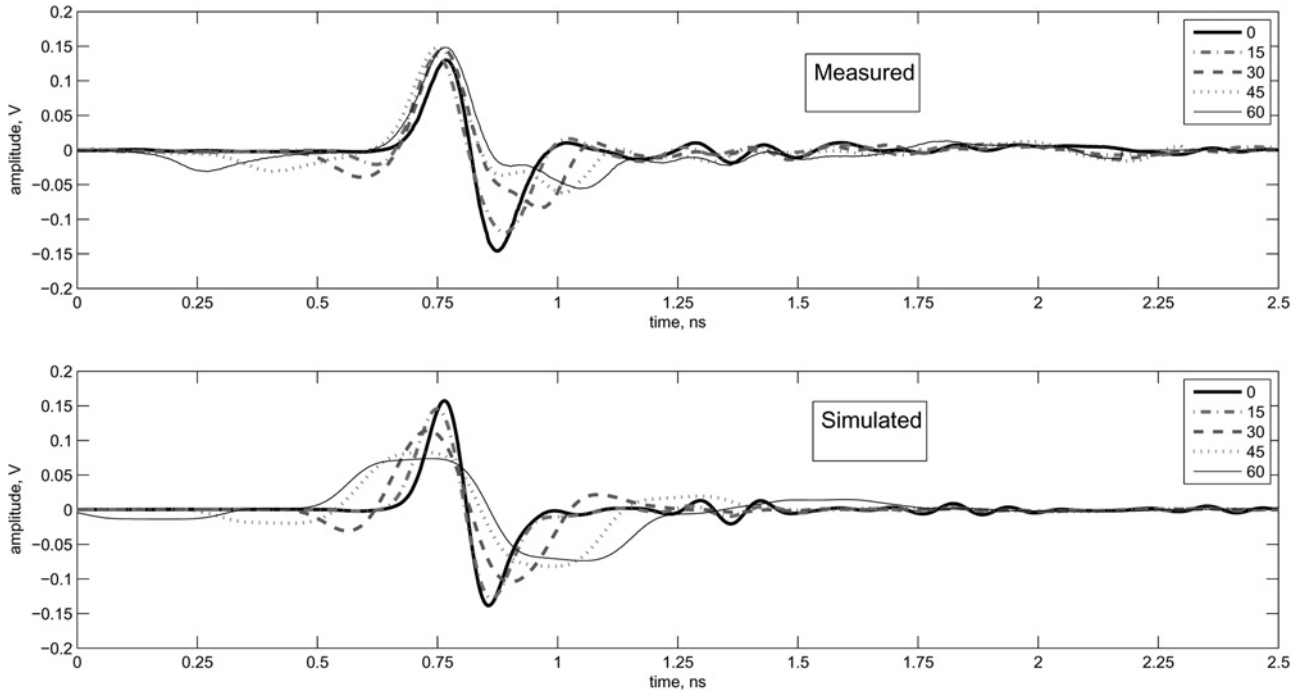

Figure 2 *Received waveforms at different receiver elevation angles, measured (above) and simulated (below)*

The templates to be deconvolved are normalised waveforms received at different angles. The duration of the templates depends on the time before the pulse decays to zero. For the templates illustrated in Fig. 2, the duration of the templates is fixed to 2.5 ns. The choice of the duration has a direct impact on the deconvolution algorithm, especially the zero-insertion case, as it determines the minimum duration between recoverable multipath components. The templates can be measured in an open environment with time gating, and no anechoic chamber is required. This allows for directional channel characterisation. Other templates can be selected for optimising the energy capture (EC). The authors in [25] took into account the distortion of pulse shape introduced by the propagation process. They used a single reference measurement in a real measurement environment. Templates were obtained manually to optimise the captured energy. This process is claimed to eliminate the 'phantom paths'. This choice is not appropriate for our directional characterisation and does not reflect physical parameters.

The methodology for performing the deconvolution process depends mainly on the objective of that process and on the judgement criteria. In channel characterisation, our goal is to find the 'best' values for the amplitude, delay and template shape (angles) such that the synthesised waveform

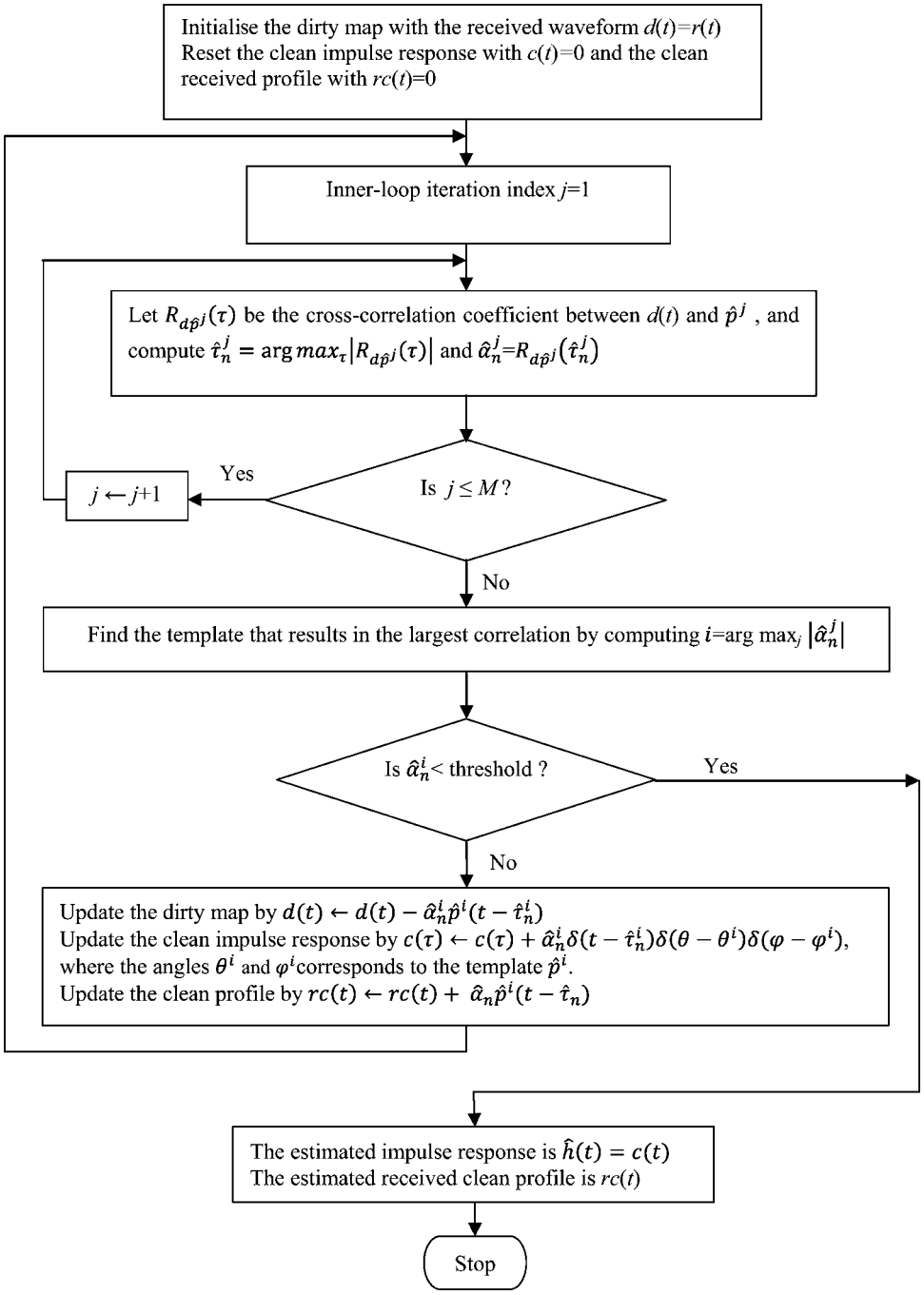

Figure 3 *Flowchart for the suggested multi-template subtractive deconvolution*

IET Commun., 2010, Vol. 4, Iss. 1, pp. 51–62
doi: 10.1049/iet-com.2008.0674

is well matched to the received waveform. The extent of achieving the goal is measured by using the EC. EC is defined as [26]

$$\mathrm{EC}(L_{\mathrm{p}}) = \left\{1 - \frac{||r(t) - rc(t)||^2}{||r(t)||^2}\right\} \times 100\% \qquad (7)$$

where L_{p} is the number of single path correlators required in the UWB Rake receiver to construct a filter matched to the received waveform, so that the constructed waveform 'adequately' captures the averaged received signal energy.

Subtractive deconvolution is used to extract the proposed model parameters where the amplitude, delay and template shape (angles) for the strongest multipath components are estimated. On the basis of the estimated parameters, the detected component is subtracted from the received profile, $r(t)$. The remainder is known as the dirty map, $d(t)$. The process continues to build a clean impulse response, $c(t)$, and a clean profile, $rc(t)$, which is made of delayed and scaled versions of the expected templates.

Assuming M different templates, the subtractive deconvolution algorithm is modified from that described in [9, 22]. The modifications support multi-templates and subtractive deconvolution rather than zero-insertion. These modifications result in improving the performance, as will be illustrated. The algorithm, which is illustrated by a flowchart in Fig. 3, starts by initialising the dirty map with the received waveform, $d(t) = r(t)$, and setting the clean impulse response and the clean received profile to zero. Next, the algorithm computes the cross-correlation coefficient between the dirty map and the M different templates, $R_{d\hat{p}^i}(\tau)$. The highest value of the cross-correlation and its time index determine the amplitude and the time delay for the first detected multipath component. The template resulting in the highest correlation, $\hat{p}^i(t)$, determines the associated angles θ^i and φ^i. The detected multipath component is then subtracted from the dirty map and added to the clean received profile. The algorithm starts

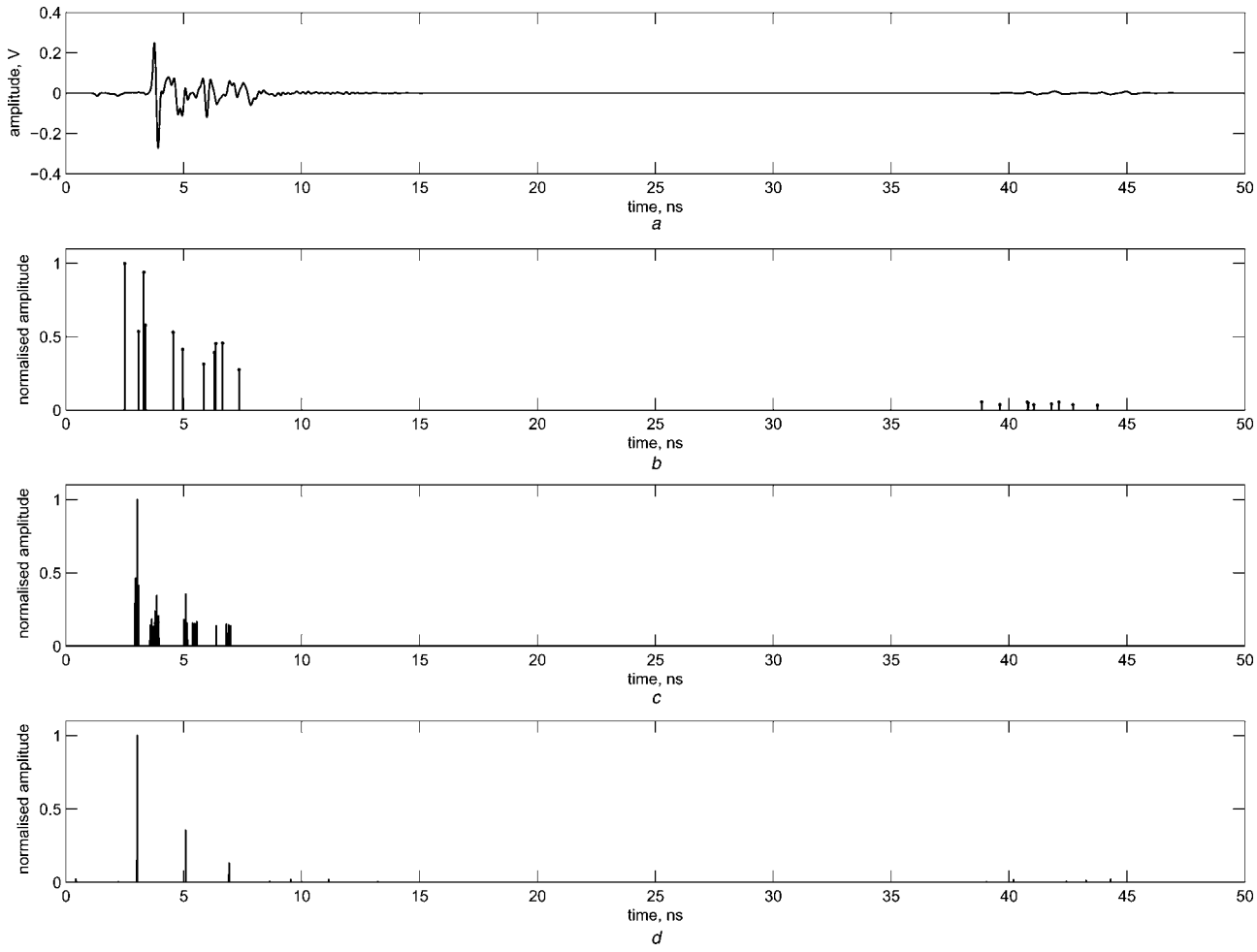

Figure 4 *Simulated example for channel impulse response recovery comparing subtractive deconvolution with zero-insertion*

a Simulated received profile
b Simulated channel taps
c Recovered channel taps using subtractive deconvolution
d Recovered channel taps using zero insertion

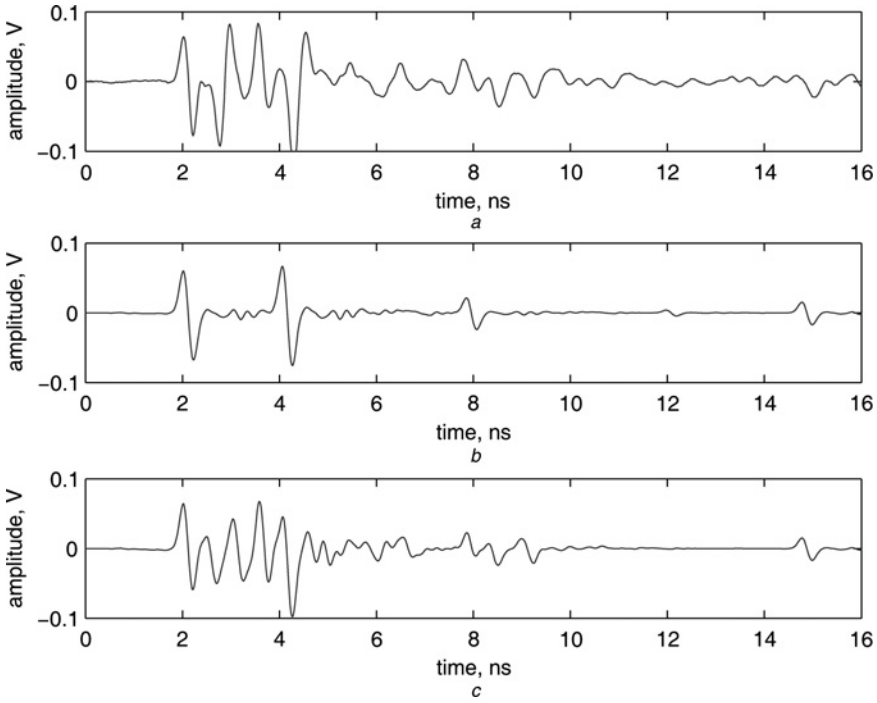

Figure 5 *Example illustrating recovery of measured signals using subtractive deconvolution vs. zero insertion*

a Measured received profile
b Reconstructed with zero-insertion
c Reconstructed with subtractive deconvolution

again by computing the cross-correlation using the updated dirty map. The process continues until all computed cross-correlations fall below a pre-specified threshold.

Note that the authors in [9] and the subsequent researchers [25, 27] updated the dirty map by inserting zeros in place of the detected component rather than by subtracting the detected components. Inserting zeros inherently assumes that multipath components do not overlap. When examining a large number of profiles, one concludes that many multipath components overlap to produce a new shape, which is the superposition of the overlapping components. To illustrate the idea, a simulated received profile is shown in Fig. 4*a*, and the associated channel taps amplitudes and delays are shown in Fig. 4*b*. The channel taps extracted by subtractive deconvolution and by zero-insertion are depicted in Figs. 4*c* and *d*, respectively. When subtractive deconvolution is used, the recovered components are concentrated around the first cluster with high energy. For the case of zero-insertion, the 20 recovered taps are spaced by at least the template duration, and some recovered taps belong to the second cluster. Utilising a single tap, both zero-insertion and subtractive deconvolution resulted in 38% EC. As we increase the number of recovered taps, the zero-insertion technique saturates around 45% of the total energy. Subtractive deconvolution recovers more than 80% of the energy with 20 taps.

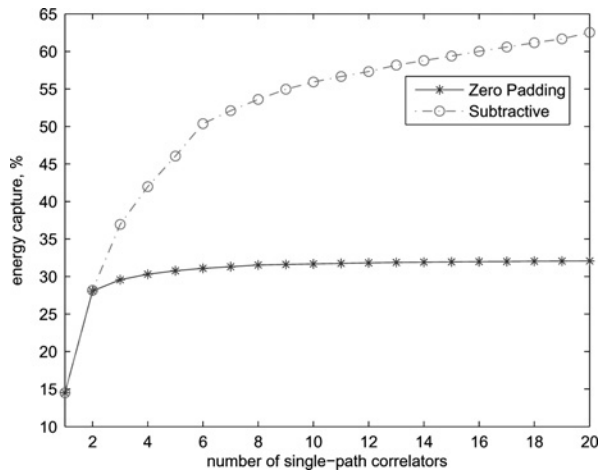

Figure 6 *Energy capture using zero-insertion and subtractive deconvolution*

The measured profiles demonstrated similar results. Fig. 5*a* illustrates a profile measured in a corridor with scatterers (walls) at similar distances from the antennas, to increase the probability of having overlapping multipath components. Using 20 multipath components, the recovered profiles with both zero-insertion and subtractive multi-template deconvolution are shown in Figs. 5*b* and *c*, respectively. It is evident from Fig. 5 that subtractive deconvolution performs better.

Fig. 6 further quantifies the improved performance. Zero-insertion has limited EC, whereas in subtractive deconvolution the EC increases monotonically as a

doi: 10.1049/iet-com.2008.0674

function of the recovered multipath components. The zero-insertion might be justified in very dispersive channels, because subtracting the template from the dispersed received profile results in a large remainder. This remainder might be mistakenly identified as a 'phantom' multipath component. On the other hand, zero-insertion, in addition to missing true multipath components, could result in 'phantom' components around the previously detected components. Counting the numbers of multipath components is not usually an objective by itself.

The deconvolution process can be terminated if a certain EC percentage is achieved or when the increment on the captured energy is below a certain threshold. Termination criteria can also be a certain number of multipath components or a specific path amplitude threshold.

In the next section, the multi-template subtractive deconvolution is applied to the measured and simulated profiles with a different number of templates.

5 Results and analysis

The energy in the measured multipath profiles is now captured by using correlators with a fixed template, and it is compared with the energy obtained by using the proposed subtractive multi-template correlators. For the multi-template case, the reference templates are based on antenna measurements at different elevation angles. Since a finite number of dominant multipath components usually exist in a typical received waveform, and since a limited number can be used by a practical Rake receiver, 20 multipath components were extracted in every profile.

Fig. 7*a* depicts the improvement in the captured energy against the number of captured multipath components. NLOS and LOS scenarios are presented separately. For each of the LOS and NLOS scenarios, the captured energy is shown by using a single template and the five suggested templates. For the case of the single template, the reference template was measured at 0°. For the case of five reference templates, the measurements were performed at the following set of elevation angles: 0°, 15°, 30°, 45°, 60°. The azimuth angle was fixed at 0°.

In both measured LOS and NLOS cases, the use of five templates resulted in about 11% increase in the captured energy. For LOS scenarios, the performance saturated with single and five templates at about 70% and 82% of the received energy, respectively. For NLOS scenarios, the performance saturated at 57% and 67% for single and five templates, respectively.

Fig. 7*b* illustrates the directional distribution of the received templates. The figure illustrates relatively high occurrence for the 60° template. It is worth noting that all arrivals with angles beyond 60° have the highest correlation with 60° templates. It was also noted in [27] that selecting the template from a typical received profile, or even using noise and random templates, results in good EC. This can be explained by noting that the aggregate effect of propagation is lowpass filtering, and the delayed components will have more low-frequency components compared to the first few arrivals. The lowpass filtering results in expanding the pulse with time, and hence the energy is distributed evenly through time and can be evenly captured by using random pulse shapes. Waveforms received at higher angles suffer from the same lowpass filtering effect, because of the characteristics of the antenna.

For the simulated profiles, the energy extraction is applied to the 200 LOS and 50 NLOS simulated profiles. The simulated templates are utilised. Similar conclusions can be drawn from Fig. 8*a* regarding the advantage of using more templates. When simulation and measurements are compared, the following points become evident. In

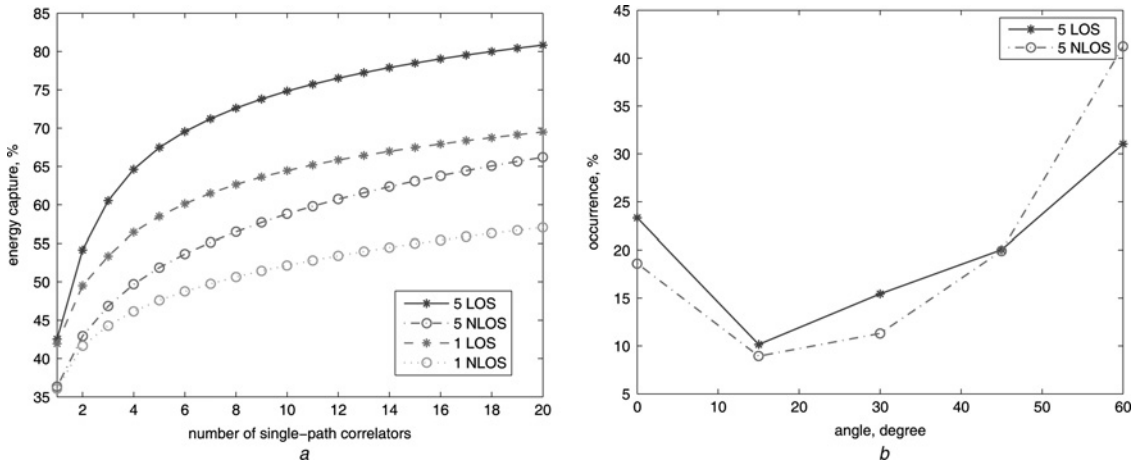

Figure 7 *Energy capture and angle distribution utilising measured profiles and templates*

a Energy capture for different number of reference templates (measured profiles and templates)
b Extracted angle distribution for LOS and NLOS scenarios (measured profiles and templates)

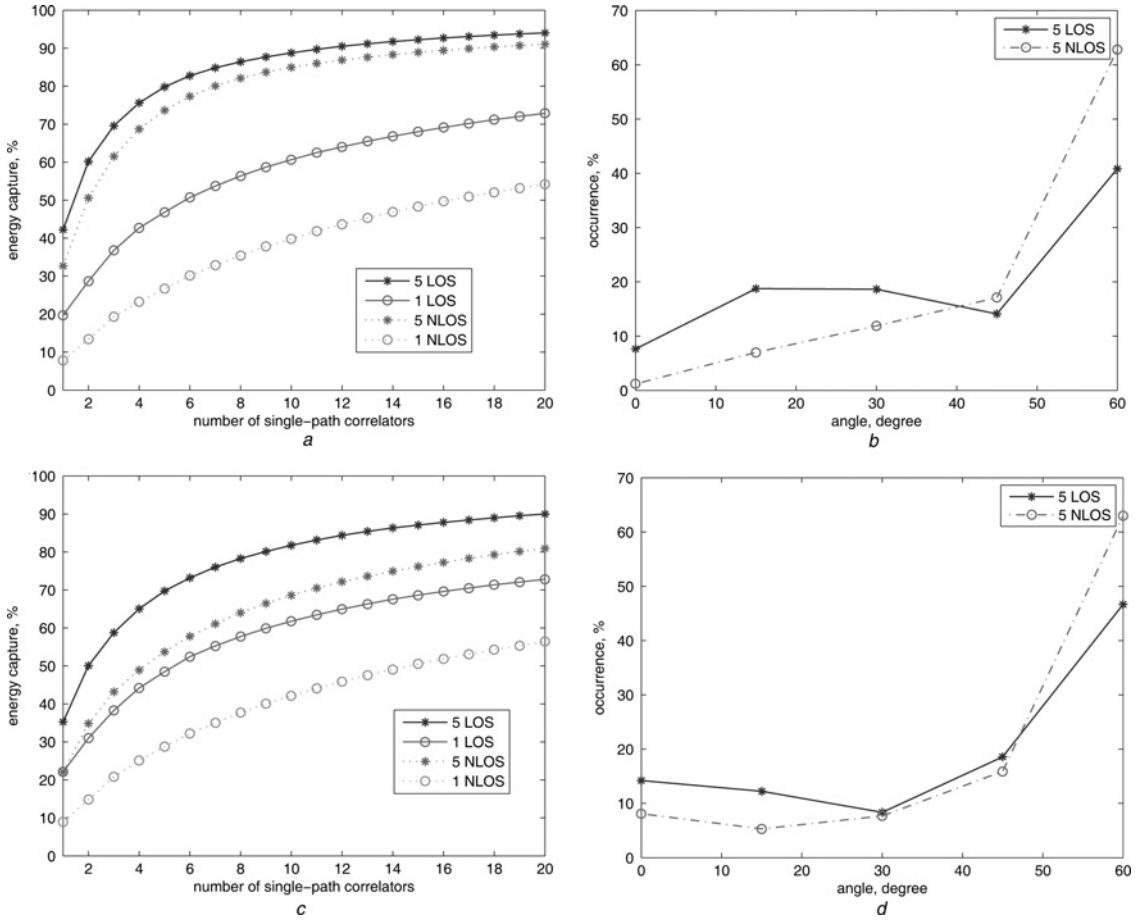

Figure 8 *Captured energy and angle distribution utilising simulated profiles and/or templates*

a Energy capture for different number of reference templates (simulated profiles and simulated templates)
b Extracted angle distribution for LOS and NLOS scenarios (simulated profiles and simulated templates)
c Energy capture for different number of reference templates (simulated profiles and measured templates)
d Extracted angle distribution for LOS and NLOS scenarios (simulated profiles and measured templates)

simulation the captured energy saturates above 90%, whereas in measurements it saturates just above 80%. This difference is expected because the simulated channel is assumed to be made of perfect reflectors, which is not the case in real measured environments.

With regard to the EC curves, the two traces for five and single templates start from the same value (at single correlator) which means that, even when five templates are used the highest energy template is always the first template (0°). This is not the case for simulation. The difference may be attributed to the mismatch between the measured environment and the used CM1 model parameters. The chosen parameters resulted in some multipath components at different angles, which have a higher correlation than the 0° case. This is also reflected in the angle distribution. Templates of 0° are fewer than templates of higher angles.

Fig. 8*b* suggests that, similar to measurements, many components from the simulated profiles are identified as having a large elevation angle of arrival. Additional multipath components support the lower frequencies of the used band.

In the last part of the simulation, we used the measured templates with the simulated profiles. As illustrated by Figs. 8*c* and *d*, less energy is captured. However, the general extracted directional distribution is not dramatically affected. This suggests that the degree of details and accuracy in representing the templates is not a major factor. Choosing and optimising the templates is still a subject for further research.

The estimated angles have limited resolution. This limitation should not detract from the novelty of the proposed technique, as it allows for direction estimation with a single UWB antenna. The estimated direction, despite its limited accuracy, could prove to be very advantageous in such applications as positioning. It could also increase the resolution of antenna arrays when the arrival is estimated by using individual elements in addition to the relative difference between the elements of the arrays.

doi: 10.1049/iet-com.2008.0674

6 Concluding remarks

In this paper, a statistical directional UWB model is proposed. The proposed model is based on the IEEE802.15.3a temporal model. The proposed model is used to develop an end-to-end UWB simulator. Moreover, a directional multi-template subtractive deconvolution is proposed and applied to an extensive UWB measurement campaign and simulated profiles. The diversity of the waveforms is utilised to extract the relative direction of arrival with a single antenna. The results obtained show that the captured energy increases by more than 10% when using the directional model with five directional correlators rather than one. The use of subtractive deconvolution, rather than zero-insertion used by previous authors, allows for the overlapping components to be resolved, and it also increases the captured energy by more than 30% when 20 correlators are used. Furthermore, angle distribution is extracted from the profiles. The angle recovery with a single antenna has a limited resolution, but it can be advantageous in many applications such as positioning. Most of the multipath components seem to preserve the low-frequency contents of the waveform. The use of the proposed directional modelling allows for many applications, and it facilitates the research in different directions such as pulse shaping studies and UWB receiver design.

7 Acknowledgments

The author acknowledges the support of the Deanship of Scientific Research at King Fahd University of Petroleum and Minerals (KFUPM) under grant/project no. FT070002. The author thanks Mr. Umar Johar and Mr. Waleed Said for their help with the simulation. The author also thanks Dr. Muhammad Taher Abuelma'atti and Mr. David Birkett for their editorial comments.

8 References

[1] ANDREWS J.: 'UWB signal sources, antennas & propagation'. IEEE Topical Conference on Wireless Communication Technology, Honolulu, Hawaii, 15–17 October 2003, pp. 439–440

[2] PANDE D.C.: 'Ultra wide band (UWB) systems and their implications to electromagnetic environment'. Proc. Int. Conf. Electromagnetic Interference and Compatibility, 1999, pp. 50–57

[3] VERDU S.: 'Wireless bandwidth in the making', *IEEE Commun. Mag.*, 2000, **38**, pp. 53–58

[4] http://www.timedomain.com, accessed October 2008

[5] ADAM J.C., GREGORWICH W., CAPOTS L., LICCARDO D.: 'Ultra-wideband for navigation and communications'. IEEE Proc. Aerospace Conf., March 2001, vol. 2, pp. 785–792

[6] MUQAIBEL A., SAFAAI-JAZI A., ATTIYA B., WOERNER B., RIAD S.: 'Pathloss and time dispersion parameters for indoor UWB propagation', *IEEE Trans. Wirel. Commun.*, 2006, **5**, (3), pp. 550–559

[7] CRAMER J.M., SCHOLTZ R.A., WIN M.Z.: 'On the analysis of UWB communication channels'. IEEE Proc. Military Communications Conf., 1999, vol. 2, pp. 1191–1195

[8] PRETTIE C., CHEUNG D., RUSCH L., HO M.: 'Spatial correlation of UWB in a home environment'. IEEE Conference on Ultra Wideband Systems and Technologies, May 2002, pp. 65–69

[9] MUQAIBEL A., SAFAAI-JAZI A., WOERNER B., RIAD S.: 'UWB channel impulse response characterization using deconvolution techniques'. 45th IEEE International Midwest Symposium on Circuits Systems, Tulsa, Oklahoma, August 2002, vol. 3, pp. 605–608

[10] MALIK W.Q.: 'Spatial correlation in ultrawideband channels', *IEEE Trans. Wirel. Commun.*, 2008, **7**, (2), pp. 604–610

[11] DABIN J., HAIMOVICH A., GREBEL H.: 'Statistical ultra-wideband indoor channel model and the effects of antenna directivity on path loss and multipath', *IEEE J. Sel. Areas Commun.*, 2006, **24**, (4), pp. 752–758

[12] LU L., GREENSTEIN J., SPASOJEVIC P.: 'Spectral and spatial properties of antennas for transmitting and receiving UWB signals', *IEEE Trans. Veh. Technol.*, 2008, **57**, (1), pp. 243–249

[13] SPENCER Q., JEFFS B., JENSEN M., SWINDLEHURST A.: 'Modeling the statistical time and angle of arrival characteristics of an indoor multipath channel', *IEEE J. Sel. Areas Commun.*, 2000, **18**, (3), pp. 347–360

[14] KLEIN A., MOHR W.: 'A tatistical wideband mobile radio channel model including the direction of arrival'. Proc. IEEE Fourth Int. Symp. Spread Spectrum Techniques and Applications, 1996, pp. 102–106

[15] SALEH A., VALENZUELA R.: 'A statistical model for indoor multipath propagation', *IEEE J. Sel. Areas Commun.*, 1987, **5**, pp. 128–137

[16] IEEE802 02/490: IEEE P802.15-02/490r0, Channel Modeling Subcommittee Final Report

[17] MUQAIBEL A., JOHAR U.: 'UWB multipath simulator based on TEM horn antenna'. Second Int. Conf. Wireless Broadband and Ultra Wideband Communications, August 2007, p. 9

[18] MOLISCH A., FOERSTER J., PENDERGRASS M.: 'Channel models for ultrawideband personal area networks', *IEEE Wirel. Commun.*, 2003, **10**, (6), pp. 14–21

[19] http://www.mathworks.com/matlabcentral/fileexchange/6697, accessed January 2009

[20] MUQAIBEL A.H.: 'Characterization of ultra wideband communication channels', PhD Dissertation, Department of Electrical and Computer Engineering, Virginia Tech., 2003

[21] MORRISON G., FATTOUCHE M.: 'Super-resolution modeling of the indoor radio propagation channel', *IEEE Trans. Veh. Technol.*, 1998, **47**, (2), pp. 649–657

[22] VAUGHAN R., SCOTT N.: 'Super-resolution of pulsed multipath channels for delay spread characterization', *IEEE Trans. Commun.*, 1999, **47**, (3), pp. 343–347

[23] PARRUCK B., RIAD S.: 'An optimization criterion for iterative deconvolution', *IEEE Trans. Instrum. Meas.*, 1983, **32**, (1), pp. 137–140

[24] NAHMAN N., GUILLAUME M.: 'Deconvolution of time domain waveforms in the presence of noise'. National Bureau of Standards, Washington, DC, Technical Notes 1047, October 1981

[25] YANG W., NAITONG Z.: 'A new multi-template CLEAN algorithm for UWB channel impulse response characterization'. Int. Conf. Communication Technology (ICCT '06), 2006, pp. 1–4

[26] WIN M., SCHOLTZ R.: 'Energy capture vs. correlator resources in ultra-wide bandwidth indoor wireless communications channels'. Proc. Military Communications Conf., 1997, vol. 3, pp. 1277–1281

[27] LIU T., KIM D., VAUGHAN R.: 'A high-resolution, multi-template deconvolution algorithm for time-domain UWB channel characterization', *Can. J. Elec. Comput. Eng.*, 2007, **32**, (4), pp. 207–213

doi: 10.1049/iet-com.2008.0674